

## Dynamics of metastable-atom deexcitation at metal surfaces

F. B. Dunning, P. Nordlander, and G. K. Walters

*Department of Physics and the Rice Quantum Institute, Rice University, P.O. Box 1892, Houston, Texas 77251*

(Received 26 December 1990; revised manuscript received 29 March 1991)

Theoretical calculations of energy levels and widths are presented that indicate that  $\text{He}(2^3S)$  atoms are sufficiently long lived near a metal surface that a significant fraction of the excited atoms contained in a thermal-energy beam can survive passage to within  $\sim 3\text{--}4 \text{ \AA}$  of the surface, where, it is suggested, Auger deexcitation might compete effectively with resonance ionization. This might account for earlier observations that electrons ejected from high-work-function metal surfaces by electron-spin-polarized  $\text{He}(2^3S)$  metastable atoms have a significant spin polarization.

Recent experiments have demonstrated that the dynamics of metastable-atom deexcitation at a surface can be explored by use of spin-labeling techniques in which electron-spin-polarized metastable atoms are directed at the target surface and the polarization of the ejected electrons is measured. Such spin-polarized metastable-atom-deexcitation spectroscopy (SPMDS) studies using thermal-energy polarized  $\text{He}(2^3S)$  metastable atoms and a variety of high-work-function clean metal surfaces have revealed that the ejected electrons have a significant spin polarization.<sup>1</sup> Conventional models<sup>2</sup> suggest that metastable atom deexcitation at a high-work-function metal surface occurs via a two-step process involving resonance ionization of the incident metastable atom followed by Auger neutralization of the resulting ion. In the neutralization process the ejected electrons originate in the metal and the observed spin polarization would require that the electrons involved in the Auger neutralization process are correlated in spin. Here we explore an alternate explanation, namely that a fraction of the incident metastable atoms do not undergo resonance ionization but rather survive passage to regions close to the surface where they undergo direct Auger deexcitation. Calculations of energy levels and widths are presented in support of this hypothesis. These calculations indicate that when a  $\text{He}(2^3S)$  atom approaches a metal surface the tunneling rate for the excited  $2s$  electron does not simply increase exponentially with decreasing atom-surface separation but rather saturates at a value of  $\sim 5 \times 10^{14} \text{ sec}^{-1}$ . This saturation results from perturbations introduced by the surface that polarize the incident atom and reduce the electron tunneling rate. Based on these calculations it is reasonable to expect that a significant fraction of the  $\text{He}(2^3S)$  atoms contained in a thermal-energy beam will approach to within  $\sim 3\text{--}4 \text{ \AA}$  from the surface where, it is argued, Auger deexcitation might become important.

The electron ejection processes that occur when a  $\text{He}(2^3S)$  atom is deexcited at a clean metal surface have been discussed by Hagstrum<sup>2</sup> and are illustrated schematically in the energy-level diagrams shown in Fig. 1. If the work function of the surface is sufficiently large, an incident atom can undergo resonant ionization (RI) through tunneling of the excited  $2s$  electron into an unfilled level above the Fermi surface in the metal, as in-

dicated by the wavy arrow in Fig. 1(a). The tunneling rate is typically assumed to increase exponentially with decreasing atom-surface separation and to be such that, at a high-work-function surface, *all* incident  $\text{He}(2^3S)$  atoms undergo RI. The resulting  $\text{He}^+$  ions continue toward the surface where they are each neutralized by a conduction electron from the metal. The released energy is imparted to a second (Auger) electron in the metal, which may, if the energy transferred is sufficiently large, be ejected from the surface. This two-electron process is termed Auger neutralization (AN). At low-work-function surfaces, RI cannot occur because there are no vacant levels of appropriate energy within the metal. In this event the  $2^3S$  atoms are deexcited by the Auger deexcitation (AD) process diagrammed in Fig. 1(b), in which an electron from the metal tunnels into the helium ground  $1s$  orbital and the energy released is communicated to the excited  $2s$  electron which may be ejected.

The ejection processes that actually occur at a given surface can be probed directly, as is evident from Figs. 1(a) and 1(b), by electron-spin polarizing the incident  $2^3S$

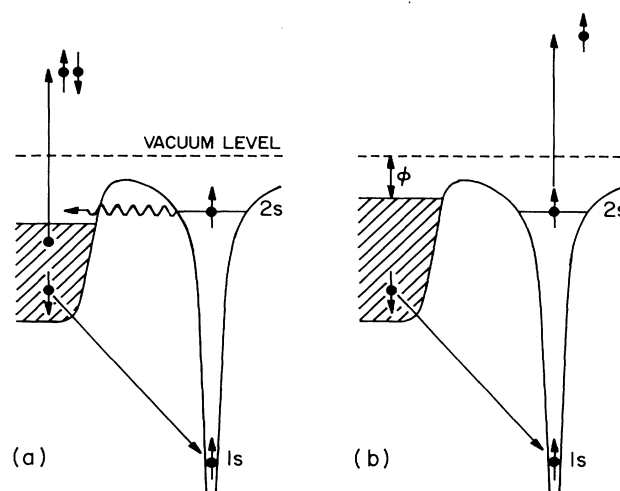


FIG. 1. Schematic diagram of the electron ejection processes that can occur when  $\text{He}(2^3S)$  atoms are deexcited at a clean metal surface.

atoms and measuring the polarization of the ejected electrons. In AD it is the excited  $2s$  electron that is ejected with polarization equal to that of the incident  $2^3S$  atoms. In contrast, in RI+AN the ejected electron originates in the surface, in which case (for nonmagnetic surfaces) the ejected-electron polarization would be zero in the absence of a spin correlation between the neutralizing and ejected electrons.

SPMDS studies of a variety of clean high-work-function metal surfaces have been undertaken in this laboratory<sup>1</sup> and show that the ejected electrons have a significant polarization. Typical data for Cu(100) are presented in Fig. 2, which shows both the ejected-electron energy distribution and energy-resolved polarization (normalized to unit incident metastable-atom polarization).<sup>3</sup> The measured average ejected-electron polarization of  $\sim 0.2$  is similar to that observed at Pd(110), (unmagnetized) Ni(110), and polycrystalline Al surfaces, and, given the possibility of secondary-electron production, must represent a lower bound to the true polarization of electrons generated in metastable-atom-surface interactions. If it is assumed that all the incident  $\text{He}(2^3S)$  atoms are deexcited exclusively by RI+AN, then the observed ejected-electron polarization implies that the electrons involved in the AN process tend to have antiparallel spins. This would require that Auger neutralization favor singlet two-hole final states in the metal target such as have been reported for certain Auger processes originating on core holes in ferromagnets.<sup>4</sup> However, the analysis below suggests that, even at high-work-function surfaces, RI+AN and AD might occur in parallel, in which case the observed spin polarization might be understood even if there were little or no spin correlation in the AN process. This possibility is discussed with reference to calculations of the energies and widths (lifetimes) of  $\text{He}(2^3S)$  atoms when near a metal surface. Shifts in the atomic energy levels occur due to changes in the electronic potential induced by the surface, and the levels broaden into resonances due to the

continuum of surface electronic states into or out of which electrons can tunnel. The present theoretical approach is similar to that described in detail elsewhere.<sup>5</sup>

Consider an excited helium atom with coordinate  $\mathbf{R}$  located outside a metal surface. The total effective potential for the excited electron, with relative coordinate  $\mathbf{r}$ , may be written

$$V^{\text{eff}}(\mathbf{r}; \mathbf{R}) = V_0^s(\mathbf{r}) + \Delta V_A^s(\mathbf{r}; \mathbf{R}) + V^A(r). \quad (1)$$

$V_0^s(\mathbf{r})$  describes the bare-electron-surface interaction. At large distances from the surface this interaction is dominated by the image force, i.e.,  $V_0^s = -1/4z$ , where  $z$  is directed outward from the surface and measured from the surface image plane. The  $\Delta V_A^s(\mathbf{r}; \mathbf{R})$  term represents the change in electron-surface potential induced by the presence of the  $\text{He}^+$  core ion, and for large  $z$  is simply the repulsive interaction between the excited electron and the image of the core ion. The image approximations to  $V_0^s$  and  $\Delta V_A^s$ , however, are not adequate for the small to intermediate values of  $z$  of interest in the present work. In particular, the image approximation to  $V_0^s$  diverges at small  $z$ , whereas the true potential should approximate that of the bulk. In order to more accurately represent  $V_0^s$  and  $\Delta V_A^s$ , the surface is described using a jellium model with parameter  $r_s = 2.65$  (this choice of  $r_s$  yields the correct local charge density  $n$  for a copper surface, where  $n = 3/4\pi r_s^3$ ).  $V_0^s$  is calculated using the weighted density approximation.<sup>6</sup>  $\Delta V_A^s$  is obtained using a linear-response approach from the surface charge distribution induced by the helium core ion.

The excited-electron-core-ion interaction is modeled by a pseudopotential of the form introduced by Simons,<sup>7</sup>

$$V_A(r) = \frac{-Z}{r} + \sum_{l=0}^{\infty} \frac{B_l P_l}{r^2}. \quad (2)$$

In this expression  $P_l$  is the projection operator for angular momentum  $l$ ,  $Z$  is the charge on the atomic core ion, and  $B_l$  is a parameter. For a single atom in vacuum, the Schrödinger equation for this potential can be solved exactly yielding the eigenvalues

$$E_v = \frac{-2Z^2}{[2n + 1 + \sqrt{(2l+1)^2 + 8B_l}]^2}. \quad (3)$$

The parameters  $B_l$  were directly determined by fitting this equation to the known triplet helium energy levels. All excited states up to those with configuration  $1s5l$  could be well reproduced by retaining only the three lowest  $l$  values in the summation in Eq. (2).

The energies and widths of the excited states are calculated directly from the Schrödinger equation using the complex scaling technique.<sup>5</sup> The wave function for a resonance state may be written simplistically as

$$\psi(t) = e^{-iEt/\hbar} \psi(t=0). \quad (4)$$

The eigenenergy  $E$  is complex and may be written  $E \equiv E_R - i\Gamma/2$ , where  $E_R$  is the real part of the energy and  $\Gamma$  is the width of the state. A Hermitian Hamiltonian, however, can produce only real eigenvalues for square-integrable eigenfunctions. The desired complex

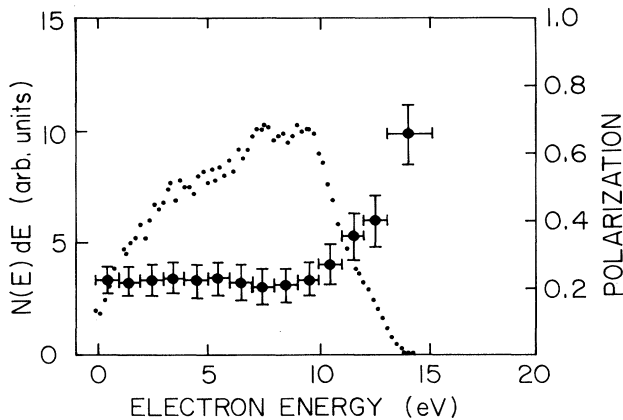


FIG. 2. Ejected-electron energy distributions (●) and energy resolved polarizations (●), normalized to unit incident metastable atom polarization, for  $\text{He}(2^3S)$  deexcitation at a clean Cu(100) surface.

eigenenergies are associated with eigenstates exhibiting so-called Siegert (diverging) boundary conditions

$$\psi(r) \xrightarrow{r \rightarrow \infty} e^{ik_R r + k_I r} f(\Omega), \quad (5)$$

where  $k_R$  and  $k_I$  are the real and imaginary parts of the complex wave number ( $k_I > 0$ ) and  $E = -(k_R + ik_I)^2/2$ . By use of the variable transformation  $\mathbf{r} \rightarrow r e^{i\theta}$  these resonance boundary conditions can be replaced by simpler bound-state conditions. Application of this complex rotation, however, results in a Hamiltonian that is both complex and non-Hermitian. The resulting one-electron Schrödinger equation is solved by expanding the eigenfunctions in a basis consisting of generalized Laguerre polynomials comprising states with values of  $n$  up to 40 and  $l$  up to 18. The matrix elements of the Hamiltonian are evaluated and the Schrödinger equation is converted into a matrix equation that is solved by direct diagonalization.

The calculated energies and widths of the helium  $2^3S$  ( $1s2s$ ) and  $2^3P$  ( $1s2p$ ,  $m=0$ ) levels are shown in Fig. 3 as a function of distance from the surface. The energies of both levels shift upwards with decreasing atom-surface separation. At large distances, the magnitude of the shifts is determined by the electron-surface potential  $V_0^s + \Delta V_A^s$  and its overlap with the atomic state. As illustrated in Fig. 1 of Ref. 5, in the vicinity of the core ion the surface potential is positive due to the repulsive-electron-core-image charge interaction  $\Delta V_A^s$ . Near the surface  $V_0^s$  dominates and the surface potential becomes negative. For a perfectly conducting metal surface the surface potential changes sign at a point one-third the distance from the surface to the atom. Near the core ion the surface potential is positive (given approximately by  $1/4z$ ) and results in an upward shift of the electron levels. These shifts are, however, different for the  $2^3S$  and  $2^3P$  states due to the greater spatial extent of the  $2^3P$

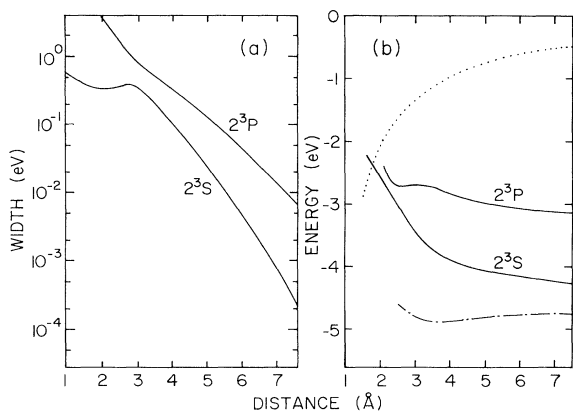


FIG. 3. (a) Calculated widths  $\Gamma$  of the He( $2^3S$ ) ( $1s2s$ ) and He( $2^3P$ ) ( $1s2p$ ,  $m=0$ ) levels near a Cu(100) surface. (b) Spatial dependence of the corresponding energy levels. The helium core-ion-surface-interaction potential is also included ( $\cdots$ ) together with an approximate total atom-surface potential ( $-\cdot-\cdot-$ ). Distances are measured from the jellium edge.

state, which extends further toward the surface and encompasses more of the region where the electron-surface potential is negative.

At intermediate atom-surface separations ( $\sim 3-4$  Å), the  $2^3S$  and  $2^3P$  levels approach each other and mixing, i.e., hybridization, of the  $2s$  and  $2p_z$  states occurs forming hybrid states that are oriented toward and away from the surface. (Calculations of the behavior of alkali atoms near metal surfaces have revealed similar hybridization.<sup>5</sup>) The effect of hybridization is illustrated for the  $2^3S$  state in Fig. 4, which shows the probability density<sup>8</sup> associated with the excited  $2s$  atomic electron at atom-surface separations of  $\sim 2.5$  and  $5$  Å. At large atom-surface separations the  $2^3S$  atomic state is largely spherically symmetric, but has a slight orientation toward the surface due to long-range image forces. At smaller separations the probability density becomes markedly asymmetric and peaks toward the vacuum. The overlap between the  $2^3S$  atom and metal states at small atom-surface separations leads to a rapid upward shift in the energy levels.

Hybridization has a pronounced effect on the electron tunneling rates, and thus on the width of the states. At large distances from the surface both the  $2^3S$  and  $2^3P$  widths show a nearly exponential increase with decreasing atom-surface separation. This is not unexpected because tunneling rates through a barrier depend exponentially on the thickness of the barrier. At smaller atom-surface separations, the  $2^3S$  width saturates at values of  $\sim 325-375$  meV, which correspond to tunneling rates of

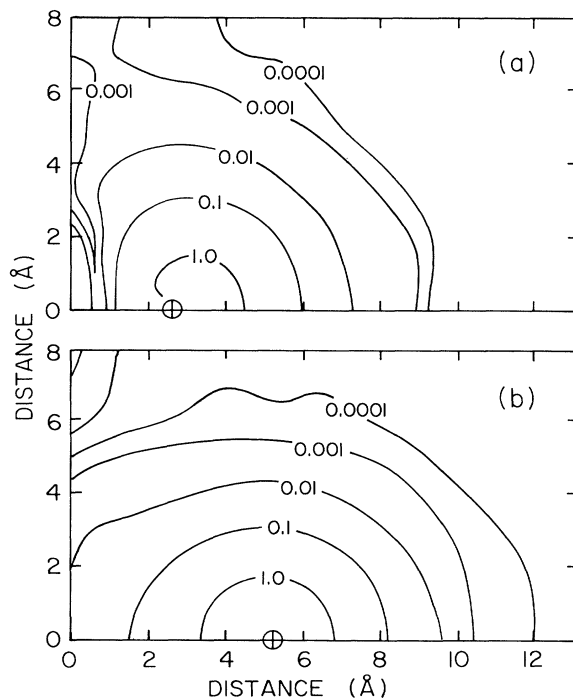


FIG. 4. Normalized probability density distributions associated with the excited  $2s$  electron at He( $2^3S$ )-surface separations of (a)  $\sim 2.5$  Å and (b)  $\sim 5$  Å. The contours are labeled in arbitrary units.

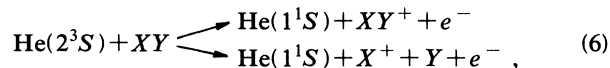
$\sim 5 \times 10^{14} \text{ sec}^{-1}$ . This saturation results because, as illustrated in Fig. 4(a), hybridization causes a marked decrease in the electron probability density in the vicinity of the barrier. In contrast, the hybrid state that derives from the  $2^3P$  level is oriented toward the surface and its width begins to increase more rapidly at the smaller atom-surface separations. Although the calculated  $2^3S$  widths are quite narrow, they are, nonetheless, somewhat larger than those measured for excited states of xenon and argon on metal surfaces using spin-resolved photoemission spectroscopy<sup>9</sup> and electron-energy-loss spectroscopy.<sup>10</sup>

The uncertainties in the calculated widths and energies are difficult to assess. The surface potential and its derivation are believed to be realistic. Similar potentials have been applied in the study of adsorbates and have provided results in good agreement with experimental measurements.<sup>11</sup> It is also assumed that the pseudopotential derived in the free-atom limit applies at small atom-surface separations. This appears reasonable, however, because the  $\text{He}^+$  core ion is very compact. Also, the general characteristics of the data shown in Figs. 3 and 4 are not sensitive to the details of the pseudopotential. The calculations do not incorporate the detailed electronic structure of the clean surface. This again should not change the general characteristics of the results. The present calculation only concerns electron tunneling, and the use of a one-electron description is inadequate when the overlap between the surface electronic wave functions and the helium  $1s$  core hole becomes sufficiently large that AD will contribute significantly to the overall level widths.

The total  $\text{He}(2^3S)$ -surface potential is difficult to calculate. A qualitative estimate can be obtained by adding the  $\text{He}^+$  core-ion-surface-interaction potential ( $V_0^s$ ) to the energy of the  $2^3S$  level. This procedure results in the total atom-surface potential shown by the dashed line in Fig. 3(b). At large distances from the surface an incident  $\text{He}(2^3S)$  atom experiences a weak attractive force. At smaller atom-surface separations, however, the interaction becomes repulsive and the atom-surface potential shown in Fig. 4(b) suggests a distance of closest approach of  $\sim 2.5 \text{ \AA}$  for an incident thermal-energy metastable atom. A more sophisticated first-principles treatment<sup>12</sup> taking into account van der Waals forces and orthogonalization suggests a somewhat smaller distance of closest approach of  $\sim 2 \text{ \AA}$ . Both treatments, however, indicate that an incident thermal-energy  $\text{He}(2^3S)$  atom can approach within  $\sim 2\text{--}2.5 \text{ \AA}$  of a clean metal surface.

The present calculated  $2^3S$  widths yield RI tunneling rates in the range  $\sim 1$  to  $5 \times 10^{14} \text{ sec}^{-1}$  at distances of  $\sim 3$  to  $4 \text{ \AA}$  from the surface. A simple estimate of the tunneling probability integrated over the incoming trajectory using the atom-surface potential shown in Fig. 3(b) suggests that  $\sim 15\%$  of the  $\text{He}(2^3S)$  atoms in a thermal-energy beam incident normally on a metal surface will survive passage to within  $4 \text{ \AA}$  from the surface. The rates associated with AD at such atom-surface separations are not known, but there is experimental evidence to suggest that they might be comparable to, if not larger than, those for RI. Specifically, spin-resolved studies of the de-

cay of xenon atoms excited at a Pt(111) surface have revealed a sizable electron signal resulting from AD.<sup>9</sup> Since the excited xenon atoms could also undergo RI, this demonstrates that AD can compete effectively with RI. (The xenon atoms were in the form of an adsorbed layer suggesting atom-surface separations of  $\sim 3 \text{ \AA}$ .) In addition, collisions of  $\text{He}(2^3S)$  atoms with gas phase targets can lead to chemi-ionization<sup>13</sup> via reactions of the type



in which the internal energy of the  $2^3S$  atom is used to ionize the target particle. Many such reactions proceed via the so-called exchange channel in which an electron from the target tunnels into the vacant  $1s$  hole in the  $2^3S$  atom with the energy liberated being used to eject the excited  $2s$  electron—a process analogous to AD. Cross sections for chemi-ionization reactions at thermal energies range from  $\sim 10$  to  $50 \text{ \AA}^2$ , which corresponds to interaction ranges of  $\sim 1.8$  to  $4 \text{ \AA}$ , indicating again that AD might be important at atom-surface separations of  $\sim 3\text{--}4 \text{ \AA}$ .

The above considerations suggest that a significant fraction of the  $\text{He}(2^3S)$  metastable atoms incident on a high-work-function metal surface might be deexcited through AD, rather than solely by RI + AN as is generally assumed. The ejected-electron polarization observed in SPMDS studies would be explained if  $\sim 20\%$  of the ejected electrons result from AD, a reasonable fraction given the uncertainties in the calculated RI tunneling rates. (The required AD fraction might actually be less than  $20\%$  since the relative escape probabilities for electrons excited in AD and AN processes may well be different. Indeed, the escape probability for electrons produced via AD might be significantly higher because the  $2s$  atomic electron is initially located outside the surface potential barrier.) Since the majority of the electron emission results from RI + AN, however, a broad relatively structureless ejected-electron energy distribution is to be expected that reflects, approximately, a self-convolution of the local density of electronic states at the surface and such a distribution is indeed observed. AD, a quasi-one-electron process, results in a narrower distribution of ejected-electron energies peaked at the higher energies. Thus contributions from AD can account for the increase in ejected-electron polarization observed at the highest ejected-electron energies. In addition, detailed comparisons between the data in Fig. 2 and the ejected-electron energy distribution measured following neutralization of low-energy  $\text{He}^+$  ions at a Cu(100) surface<sup>14</sup> show that, although both distributions display similar general characteristics, the relative number of high-energy electrons appears greater in the metastable-atom data.

The preceding discussions suggest that the SPMDS data might be explained if some of the incident metastable atoms undergo AD. A number of experimental tests of this hypothesis appear possible. The most direct is simply to measure the polarization of electrons ejected by an incident beam of polarized  $\text{He}^+$  ions; if this polarization is zero, then the polarization observed in SPMDS

studies must be associated with AD. An alternate approach is to use a beam of fast polarized He( $2^3S$ ) atoms (with energies of a few to several tens of electron volts) and measure the polarization of the ejected electrons as a function of He( $2^3S$ ) atom velocity. As the velocity increases, a greater fraction of the incident atoms will survive passage to regions close to the surface, and the distance of closest approach to the surface will decrease. Since both of these effects will increase the relative importance of AD, an increase in ejected-electron polarization should occur. It is interesting to note that SPMDS studies have already shown that the average polarization of electrons ejected by (thermal-energy) polarized

Ne( $^3P_2$ ) and Ar( $^3P_2$ ) metastable atoms from a Pd(110) surface is a factor of 2 smaller than that observed, at the same surface, using polarized He( $2^3S$ ) atoms.<sup>1</sup> This observation might be explained by noting that the lower velocities associated with the heavier metastable atoms would increase the probability of RI during the approach to the surface.

This research is supported by the Office of Basic Energy Sciences, U.S. Department of Energy, the Robert A. Welch Foundation, and the Donors of the Petroleum Research Fund administered by the American Chemical Society.

<sup>1</sup>M. W. Hart, M. S. Hammond, F. B. Dunning, and G. K. Walters, *Phys. Rev. B* **39**, 5488 (1989).

<sup>2</sup>H. D. Hagstrum, in *Electron and Ion Spectroscopy of Solids*, edited by L. Furmans, J. Vennick, and W. Dekeyser (Plenum, New York, 1978), p. 278.

<sup>3</sup>The He( $2^3S$ ) polarization is defined as  $P_z = (n_{+1} - n_{-1}) / (n_{+1} + n_0 + n_{-1})$  where  $n_{+1}$ ,  $n_0$ , and  $n_{-1}$  are the populations in the  $M_J(M_s) = 1, 0,$  and  $-1$  magnetic sublevels. The ejected electron polarization is  $P = (n_{\uparrow} - n_{\downarrow}) / (n_{\uparrow} + n_{\downarrow})$  when  $n_{\uparrow}$  and  $n_{\downarrow}$  are the numbers of spin-“up” ( $m_s = \frac{1}{2}$ ) and -“down” ( $m_s = -\frac{1}{2}$ ) electrons, respectively.

<sup>4</sup>R. Allenspach, D. Mauri, M. Taborelli, and M. Landolt, *Phys. Rev. B* **35**, 4801 (1987).

<sup>5</sup>P. Nordlander and J. C. Tully, *Phys. Rev. B* **42**, 5564 (1990).

<sup>6</sup>S. Ossicini, C. M. Bertoni, and P. Gies, *Europhys. Lett.* **1**, 661 (1986).

<sup>7</sup>G. Simons, *J. Chem. Phys.* **55**, 756 (1971).

<sup>8</sup>The wave function of a resonance state diverges asymptotically. A qualitative representation of the wave function is obtained by analytically continuing the resonance wave function to  $\theta = 0$ . The wave function so obtained is normalizable.

<sup>9</sup>G. Schönhense, A. Eyers, and U. Heinzmann, *Phys. Rev. Lett.* **56**, 512 (1986).

<sup>10</sup>J. E. Demuth, Ph. Avouris, and S. Schmeisser, *Phys. Rev. Lett.* **50**, 600 (1983); D. Schmeisser, C. M. Weinert, Ph. Avouris, and J. E. Demuth, *Chem. Phys. Lett.* **104**, 263 (1984).

<sup>11</sup>P. Nordlander and J. C. Tully, *Surf. Sci.* **211/212**, 207 (1989).

<sup>12</sup>P. Nordlander and J. Harris, *J. Phys. C* **17**, 1141 (1984).

<sup>13</sup>A. J. Yench, in *Electron Spectroscopy: Theory, Techniques and Applications*, edited by C. R. Brundle and A. D. Baker (Academic, New York, 1984), Vol. 5.

<sup>14</sup>H. D. Hagstrum, P. Petrie, and E. E. Chaban, *Phys. Rev. B* **38**, 10264 (1988).